

# Single-cycle electromagnetic pulses produced by oscillating electric dipoles

Zhaoying Wang and Qiang Lin

*Institute of Optics and State Key Laboratory of Modern Optical Instrumentation, Zhejiang University, Hangzhou 310028, China*

Zhongyang Wang

*Shanghai Institute of Optics and Fine Mechanics, Chinese Academy of Science, Shanghai 201800, China*

(Received 5 April 2002; revised manuscript received 1 October 2002; published 29 January 2003)

We report an exact analytic solution of the Maxwell equations that is capable of describing single-cycle electromagnetic pulses beyond the slowly varying envelope approximation. The solution is based on the radiation field emitted by oscillating electric dipoles under the complex-source-point model. The spatiotemporal evolution of single-cycle electromagnetic pulses in free space is illustrated and discussed in detail by using the analytic solution obtained.

DOI: 10.1103/PhysRevE.67.016503

PACS number(s): 41.60.-m, 03.50.De, 78.20.Bh

## I. INTRODUCTION

Recent developments in laser technology have resulted in the generation of extremely short and intense laser pulses, containing only a few optical cycles [1–3], even only one cycle [4] and one-half cycle [5] at optical frequencies. Much attention is therefore being paid to the problem of ultrashort pulse propagation in vacuum, dispersive linear or nonlinear media, and complicated optical systems. If the pulse duration is much larger than the optical cycle, the pulse evolution is governed by an effective parabolic three-dimensional nonlinear Schrödinger equation under the slowly varying envelope approximation (SVEA) [6]. By all appearances this approximation cannot be applied to single-cycle pulses. In fact, the SVEA breaks down in the self-focusing and self-steepening of a femtosecond optical pulse long before the pulse duration approaches the carrier oscillation cycle [7–10].

Recently, the evolution of single-cycle electromagnetic pulses has attracted even more attention. Hellwarth and Nouchi [11] derived the vector electromagnetic field components from a complex Hertz potential  $\hat{z}f(\vec{r}, t)$  oriented in the direction of wave propagation. The real and imaginary parts of the scalar generating function  $f(\vec{r}, t)$  are solutions of the scalar wave equation in vacuum. Hunsche *et al.* [12] investigated experimentally and calculated numerically the properties of single-cycle terahertz pulses propagating through an aplanatic lens. Feng *et al.* [13] derived solutions of Maxwell's equations for a transversely oriented Hertz vector to describe focused single-cycle electromagnetic pulses. These finite energy solutions are a subset of Ziolkowski's modified power spectrum pulse solutions [14].

In contrast to previous work, we present a different approach to studying the evolution of a single-cycle electromagnetic pulse beyond the slowly varying envelope approximation in the spatial-temporal domain in this paper. Our approach is based on the electromagnetic field emitted by oscillating electric dipoles. The electromagnetic field is an exact analytic solution of the Maxwell equations. Therefore, no slowly varying envelope approximation is required. We assume the oscillation of the electric dipole is of Gaussian shape. The complex-source-point model is used to remove the singular point at the origin of the coordinates.

## II. ELECTROMAGNETIC FIELD OF ELECTRIC DIPOLES

Let us assume a pair of electric dipoles in vacuum. The negative charge  $-q$  is fixed at the origin of the coordinates, while the positive charge  $+q$  is located along the  $x$  axis and is oscillating with time. Thus the time-varying electric dipole moment can be written as

$$\vec{p}(t) = ql(t)\vec{e}_x, \quad (1)$$

where  $l(t)$  is the distance between the negative and positive charges and  $\vec{e}_x$  is the unit vector along the  $x$  axis. The vector potential of the electric dipole radiation field is given by [15]

$$\vec{A}(x, y, z, t) = \frac{\mu_0}{4\pi} \int_V \frac{\vec{j}(t-R/c)}{R} dV' = \frac{\mu_0}{4\pi R} [\dot{p}] \vec{e}_x, \quad (2)$$

where  $\vec{j}$  is the electric current density vector,  $R = \sqrt{x^2 + y^2 + z^2}$  is the distance from the origin of coordinates to the observation point,  $c$  is the velocity of light in vacuum,  $t-R/c$  is the retarded time, and  $[\dot{p}]$  represents the first partial derivative of the electrical dipole moment  $p$  with respect to the retarded time  $(t-R/c)$ . In the following, the time factor of each physical quantity written in shortened form with brackets indicates the retarded time. Under the Lorentz condition  $\vec{\nabla} \cdot \vec{A} + \partial\varphi/\partial(c^2t) = 0$ , we can derive the expression for the scalar potential as follows:

$$\varphi(x, y, z, t) = -\frac{c^2\mu_0}{4\pi} \left\{ -\frac{x}{cR^2} [\dot{p}] - \frac{x}{R^3} [p] \right\}. \quad (3)$$

Using the relations between the electromagnetic field and the potential function

$$\vec{E} = -\vec{\nabla}\varphi - \partial\vec{A}/\partial t, \quad (4)$$

$$\vec{B} = \vec{\nabla} \times \vec{A}, \quad (5)$$

the following expressions for the electric dipole radiation field can be obtained [16]:

$$\begin{aligned} \vec{E}(x,y,z,t) = & -\frac{c^2\mu_0}{4\pi} \left\{ \frac{[\ddot{p}]}{c^2R} + \frac{[\dot{p}]}{cR^2} + \frac{[p]}{R^3} \right\} \vec{e}_x + \frac{c^2\mu_0}{4\pi} \frac{x}{R^2} \\ & \times \left\{ \frac{[\dot{p}]}{c^2R} + \frac{3[\ddot{p}]}{cR^2} + \frac{3[\dot{p}]}{R^3} \right\} (x\vec{e}_x + y\vec{e}_y + z\vec{e}_z), \end{aligned} \quad (6)$$

$$\vec{H}(x,y,z,t) = -\frac{c}{4\pi R} \left\{ \frac{[\dot{p}]}{c^2R} + \frac{[\ddot{p}]}{cR^2} \right\} (z\vec{e}_y - y\vec{e}_z), \quad (7)$$

where  $[\dot{p}]$  and  $[\ddot{p}]$  represent the first and second order partial derivatives of the electrical dipole moment  $p$  with respect to the retarded time.

There is a singular point at  $R=0$  in Eqs. (6) and (7). In order to remove the singular point, we use the complex-source-point model, which was first introduced for scalar beams by Deschamps [17]. The basic idea of the complex-source-point model is as follows.

Assuming an oscillation source point placed at the center of real-space coordinates  $(0,0,0)$ , it can radiate the spherical wave field

$$E(R) = \exp(ikR)/R, \quad (8)$$

which is the rigorous solution of the wave equation. The point  $R=0$  is a singularity. To avoid the singularity, the location of the oscillation source point is assigned the point  $C(0,0,-iz_0)$ , and then  $R$  becomes complex,  $R = \sqrt{x^2 + y^2 + (z + iz_0)^2}$ . In the complex-source-point model, the spherical wave field remains a rigorous solution of the wave equation [18,19]. Under the paraxial approximation,  $R$  becomes  $R = z + iz_0 + (x^2 + y^2)/2(z + iz_0)$ . Substituting  $R$  into Eq. (8), one obtains the Gaussian beam field [17].

The complex-source-point method has also been applied to other beams. For example, Siegman proposed complex Hermite-Gaussian wave functions [20]; Ziolkowski obtained Gaussian pulses by assuming a complex source point moving at a constant speed parallel to the real axis of propagation [21]; Cullen and Yu provided an exact theory for an open resonator having mirrors of a specific nonspherical shape [19]. Recently, Sheppard and Saghafi used this simple mathematical form to analyze the electromagnetic wave beyond the slowly varying envelope approximation. They discussed the beam mode for an electric dipole sink and source pair oriented along the  $x$  axis that is a rigorous solution of Maxwell's equations [22–24].

Now we replace  $z$  and  $R$  by  $z'$  and  $R'$ , respectively, in the expressions for the electric dipole radiation field Eqs. (6) and (7) through

$$z' = z + iz_0, \quad R' = \sqrt{x^2 + y^2 + (z + iz_0)^2}, \quad (9)$$

where  $z_0 = \pi w_0^2/\lambda$  represents the Rayleigh range, and  $w_0$  is the size of the beam waist. According to the resonator theory, the Rayleigh range is a constant for components of the field with various frequencies. It does not depend on the wavelength, but is only determined by the parameters of the cavity [25]. Only when  $z=0$  and  $\sqrt{x^2 + y^2} = z_0$  does  $R'$  vanish. To overcome this deficiency, we choose the Rayleigh range that

satisfies the condition  $z_0 > \sqrt{x^2 + y^2}$  on the plane of  $z=0$ . This condition is satisfied as long as the beam spot size not much smaller than the wavelength. This condition also exists for a spherical wave with a complex source point [17] and the field radiated from an impulsive source at a complex-source-point location [26].

It can be verified that in the complex-source-point model the electric dipole radiation fields still satisfy Maxwell's equations exactly in spite of the oscillating form of the electric dipoles. The verification procedure is provided in the Appendix. The field is capable of describing single-cycle electromagnetic pulses beyond the slowly varying envelope approximation. As we are considering the propagation properties of single-cycle pulses in free space, it is unnecessary to include the source terms of Maxwell's equations.

### III. SINGLE-CYCLE ELECTROMAGNETIC PULSES

Now we assume a pair of electric dipoles that oscillates with time in free space. The envelope of the oscillation amplitude is also a function of time, which is assumed to be of Gaussian shape for the sake of simplicity. Under the complex-source-point model, the electric moment of the electric dipoles can be expressed as

$$[\vec{p}] = ql_0 \exp\left[-\frac{(t-R'/c)^2}{2T^2}\right] \exp[i\omega_0(t-R'/c)] \vec{e}_x, \quad (10)$$

where  $\omega_0 = k_0c$  is the central angular frequency of the pulse and  $k_0$  is the wave number in vacuum. The full width at half maximum (FWHM) of the envelope is  $2\sqrt{2\ln 2}T$ . Substituting Eq. (10) into Eqs. (6) and (7), we obtain the exact expressions for the electric and magnetic fields of the electromagnetic pulses emitted by the electric dipoles in free space:

$$\begin{aligned} \vec{E}(x,y,z,t) = & \frac{c^2\mu_0}{4\pi} \frac{[p]}{R'} \left\{ -(f_1 + f_2i)\vec{e}_x \right. \\ & \left. + \frac{x}{R'^2} (f_3 + f_4i)(x\vec{e}_x + y\vec{e}_y + z'\vec{e}_z) \right\}, \end{aligned} \quad (11)$$

$$\vec{H}(x,y,z,t) = -\frac{c}{4\pi} \frac{[p]}{R'^2} \left\{ f_1 - \frac{1}{R'^2} + f_2i \right\} (z'\vec{e}_y - y\vec{e}_z), \quad (12)$$

where

$$f_1 = \frac{(R' - ct)^2}{c^4 T^4} - \frac{t}{c T^2 R'} + \frac{1}{R'^2} - k_0^2, \quad (13)$$

$$f_2 = \frac{2k_0(R' - ct)}{c^2 T^2} + \frac{k_0}{R'}, \quad (14)$$

$$f_3 = \frac{(R' - ct)^2}{c^4 T^4} - \frac{3t}{c T^2 R'} + \frac{3}{R'^2} + \frac{2}{c^2 T^2} - k_0^2, \quad (15)$$

$$f_4 = \frac{2k_0(R' - ct)}{c^2 T^2} + \frac{3k_0}{R'}. \quad (16)$$

As a direct consequence of Maxwell's equations, the Poynting vector of the ultrashort electromagnetic pulse can be expressed as follows:

$$\vec{S}(x, y, z, t) = \text{Re}[\vec{E}(x, y, z, t)] \times \text{Re}[\vec{H}(x, y, z, t)], \quad (17)$$

where "Re" represents the real part of a complex quantity.

The factor  $(t - R'/c)$  in Eqs. (13)–(16) represents retarded time if  $R'$  is a real quantity. Under the complex-source-point model,  $R' = \sqrt{x^2 + y^2 + (z + iz_0)^2}$  is complex. The Rayleigh range  $z_0$  appears not only in the amplitude part but also in the phase part of the electromagnetic fields. From Eqs. (11) and (12), we can see that the spatial and temporal parts are coupled.

If the full width at half maximum of the envelope approaches infinity, our solution will go back to previous results [22]. Assuming  $T \rightarrow \infty$ , then Eqs. (13)–(16) become

$$f_1 \approx 1/R'^2 - k_0^2, \quad f_2 \approx k_0/R', \quad (18)$$

$$f_3 \approx 3/R'^2 - k_0^2, \quad f_4 \approx 3k_0/R'. \quad (19)$$

Substituting Eqs. (18) and (19) into Eqs. (11) and (12), we can obtain the electromagnetic field produced by the time-harmonic oscillating dipoles. The results are the same as those of Ref. [22], where the beams produced by the time-harmonic electric and magnetic dipoles were considered.

From Eqs. (11)–(16), we can see that the expressions for the electromagnetic field are very complicated. It is difficult to reveal the evolution properties analytically via these equations. Nevertheless, we can analyze the characteristics of the electric dipole moment instead of the electromagnetic field. Setting  $t=0$ ,  $z=0$  in Eq. (10), we can get the transverse distributions of the dipole moment as follows:

$$[p] = ql_0 \exp\left[\frac{z_0^2}{2c^2T^2}\right] \exp\left[-\frac{x^2 + y^2}{2c^2T^2}\right] \exp\left[k_0\sqrt{z_0^2 - (x^2 + y^2)}\right]. \quad (20)$$

From Eq. (20), we can see that the envelope of the electric dipole moment is of Gaussian shape. The shape of the electromagnetic field is determined by the transverse distribution of the electric dipole moment. We can see in the following calculations that the electromagnetic field is also Gaussian in shape.

Now we illustrate the propagation properties of the electromagnetic field with some numerical calculations. The electric field distribution in spatial coordinates can be calculated based on Eq. (11). In the calculations, the parameters are chosen as  $\lambda_0 = 1064$  nm,  $w_0 = 0.8\lambda_0$ , and the time  $t = 1.5$  fs. Figures 1(a) and 1(b) show the distributions of the square of the electric field envelope  $|\vec{E}|^2$  versus the  $x$  coordinate when the pulse width (FWHM) equals 3.5 and 35 fs, respectively. The longitudinal coordinates in Figs. 1(a) and 1(b) are normalized to the maximum value. Because the electromagnetic field is almost symmetric in  $x$  and  $y$  coordinates, we only draw the distribution versus the  $x$  coordinate. Comparing Fig. 1(a) with Fig. 1(b), we see that the square of the electric field envelope  $|\vec{E}|^2$  keeps its Gaussian shape dur-

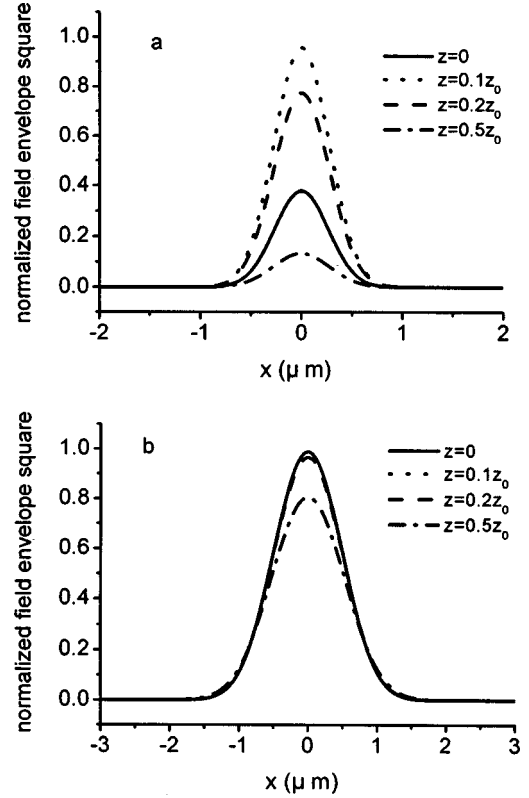


FIG. 1. Distributions of the square of the electric field envelope for the electromagnetic pulse versus  $x$  coordinate.  $2\sqrt{2} \ln 2T =$  (a) 3.5 and (b) 35 fs.

ing propagation in space and the amplitude oscillates with the propagation distance. The speed of oscillation of the amplitude with the propagation distance of a multicycle pulse is slower than that of a single-cycle pulse.

The Poynting vector of an ultrashort electromagnetic pulse can be calculated based on Eq. (17). Figures 2(a) and 2(b) show the distributions of the instantaneous energy density versus the  $x$  coordinate when the pulse width (FWHM) equals 3.5 and 35 fs, respectively. The parameters  $\lambda_0$ ,  $w_0$ , and  $t$  used in the calculation are the same as in Fig. 1. The longitudinal coordinates in Figs. 2(a) and 2(b) are normalized to the maximum value. From Fig. 2, we can see that the electromagnetic pulse produced by oscillating electric dipoles propagates mainly along the  $z$  axis. The shape of the instantaneous energy density remains invariant during the propagation in space. The amplitude of the instantaneous energy density oscillates with the propagation distance. These properties are similar to those of the focused single-cycle electromagnetic pulse given in Ref. [13]. Comparing Fig. 2(a) with Fig. 2(b), we see that the change of the amplitude of oscillation of a multicycle pulse with propagation distance is more rapid than that of a single-cycle pulse.

From Figs. 1 and 2, we can see that the square of the electric field envelope and the instantaneous energy density are different. These differences are caused by the following effects. Initially, the square of the electric field envelope does not include the phase factor. But we can see from Eq. (17) that the instantaneous energy density is modulated by a phase factor. Secondly, the pulse width and the oscillation

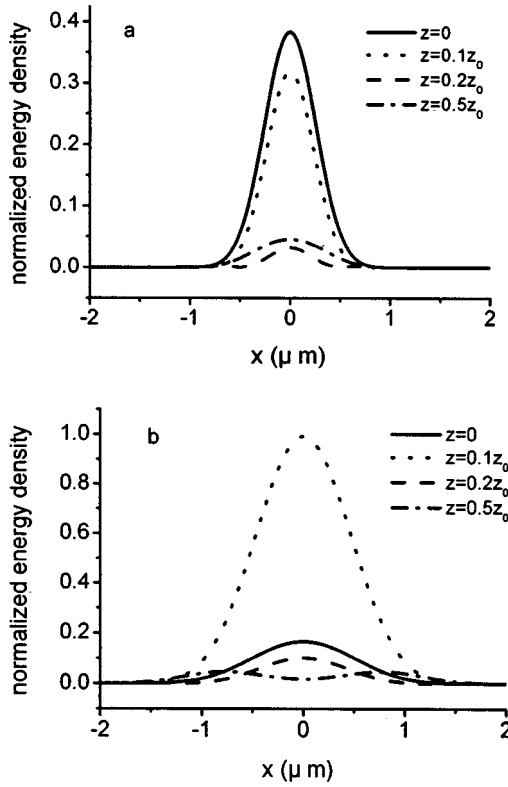


FIG. 2. Distributions of the instantaneous energy density for the electromagnetic pulse versus  $x$  coordinate.  $2\sqrt{2} \ln 2T =$  (a) 3.5 and (b) 35 fs.

frequency of the multicycle pulse are larger than those of a single-cycle pulse. Their propagation velocity is the same as the velocity of light in vacuum. The spatial distribution of the instantaneous energy density of the multicycle pulse is more complicated than that of the single-cycle pulse. And the speed of amplitude oscillation of the electric field envelope squared changes with propagation distance for a single-cycle pulse faster than for a multicycle pulse. These properties can be obtained from the following analysis of the temporal evolution.

Next let us discuss the temporal evolution of single-cycle pulses. From Eq. (10) the electrical dipole moment on the  $z$  axis ( $x=0, y=0$ ) can be expressed as

$$[\vec{p}] = ql_0 \exp\left(\frac{\pi^2 w_0^4}{2\lambda_0^2 c^2 T^2} + k_0 z_0\right) \exp\left[-\frac{(t-z/c)^2}{2T^2}\right] \times \exp\left[i\omega_0\left(1 + \frac{w_0^2}{2c^2 T^2}\right)\left(t - \frac{z}{c}\right)\right] \vec{e}_x. \quad (21)$$

From Eq. (21) we can see that the oscillation angular frequency of the electric dipole moment is  $\omega_0[1 + w_0^2/(2c^2 T^2)]$  instead of  $\omega_0$ . That is to say, the Gaussian beam waist  $w_0$  affects not only the amplitude but also the frequency. With the increase of the beam waist  $w_0$ , the angular frequency increases.

The temporal evolution of a single-cycle electromagnetic pulse for different values of propagation distance can be calculated based on Eq. (17). The results are drawn in Fig. 3. In

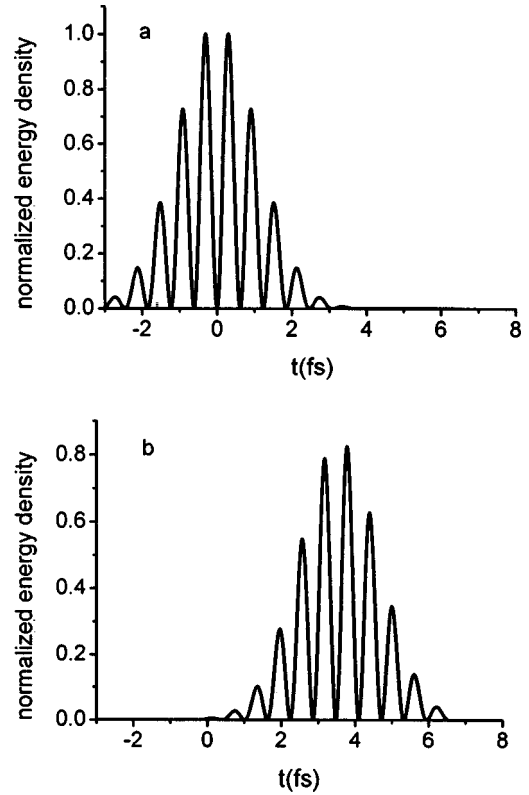


FIG. 3. Distributions of the instantaneous energy density of a single-cycle electromagnetic pulse versus time  $t$ .  $z =$  (a) 0 and (b)  $0.5z_0$ .

the calculation, we assumed the wavelength  $\lambda_0 = 1064$  nm, beam waist  $w_0 = 0.8\lambda_0$ , and pulse width (FWHM) of 3.5 fs. Figure 3 shows the distributions of the instantaneous energy density versus time  $t$  when  $z =$  (a) 0 and (b)  $0.5z_0$ . The longitudinal coordinates of Fig. 3 have the same meaning as in Fig. 2. From Fig. 3, we can see that the single-cycle electromagnetic pulse propagates mainly along the  $z$  axis at the speed of light in vacuum. On the plane of  $z = 0$ , the pulse is symmetric and the center of the pulse is located at  $t = 0$ . With increase of the propagation distance, the pulse becomes asymmetric and the center is located at  $t = z/c$ . It is caused by the derivative of the pulse with respect to the retarded time  $(t - z/c)$  [27]. During propagation, the pulse duration remains invariant. The instantaneous energy density does not oscillate with time in a harmonic form; its amplitude forms an envelope with Gaussian shape. If the pulse width increases, the envelope shape of the energy density remains invariant but the oscillation frequency increases.

The amplitude of the longitudinal coordinate at the instantaneous time  $t = 1.5$  fs in Fig. 3 is connected with the corresponding number in Fig. 2(a). We can see that with the pulse propagating along the  $z$  axis, the amplitude at  $t = 1.5$  fs oscillates. This result is consistent with Fig. 2(a). The transmission characteristics of the energy density for different values of the propagation distance as shown in Fig. 3 are the same as in Ref. [14], where a different method was used. It confirms that the methods used in this paper are correct.

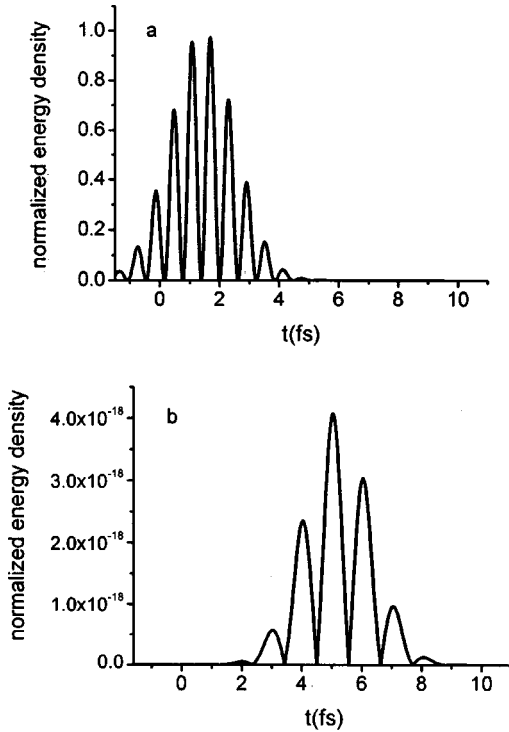


FIG. 4. Distributions of the instantaneous energy density of a single-cycle electromagnetic pulse versus time  $t$  at  $z=0.2z_0$ .  $x=(a) 0$  and  $(b) 3w_0$ .

Figure 4 shows the distributions of the instantaneous energy density versus time  $t$  based on Eq. (17) when  $x=(a) 0$  and  $(b) 3w_0$ . The parameters used in the calculation are  $\lambda_0=1064$  nm,  $w_0=0.8\lambda_0$ ,  $z=0.2z_0$ , and the pulse width (FWHM) is 3.5 fs. The longitudinal coordinates are normalized to the maximum value. From Fig. 4, we can see that with the increase of the lateral coordinate  $x$  the pulse width of the single-cycle electromagnetic wave expands in time. For different beam waists the expansion velocity of the electromagnetic pulse is different. The temporal expansion speed is faster when the beam waist is smaller. The location of the pulse maximum is shifted to higher values of time  $t$  when the lateral coordinate  $x$  increases.

#### IV. CONCLUSIONS

We presented an exact solution of Maxwell's equations that is capable of describing single-cycle electromagnetic pulses. In order to remove the singular points, we used the complex-source-point model. The spatiotemporal evolution of a single-cycle electromagnetic pulse beyond the slowly varying envelope approximation has some unique propagation properties in free space. Initially, the square of the electric field envelope  $|\vec{E}|^2$  remains in Gaussian shape during propagation in space, but the amplitude oscillates as the propagation distance increases. The evolution of the instantaneous energy density is similar. Second, the single-cycle electromagnetic pulse width and pulse shape remain invariant during the propagation. The instantaneous energy density does not oscillate with time in a harmonic form; its ampli-

tude forms an envelope with Gaussian shape. If the pulse width increases, then the oscillating frequency of the energy density increases. Third, with increase of the lateral coordinate  $x$ , the single-cycle electromagnetic pulse expands in time. The temporal expansion speed is faster when the beam waist is smaller. The location of the pulse maximum is shifted to higher values of time  $t$  when the lateral coordinate  $x$  increases.

#### ACKNOWLEDGMENTS

This work is supported by the National Natural Science Foundation of China (Grant No. 60078003), the Youth Teacher Foundation of the Huo Ying Dong Education Foundation of China (Grant No. 71009), and the Zhejiang Provincial Natural Science Foundation of China (Grants No. RC98029 and No. 601137).

#### APPENDIX

In this appendix we show that, in the complex-source-point model, the electric dipole radiation fields still satisfy Maxwell's equations exactly in spite of the oscillating form of the electric dipoles.

We replace  $z$  and  $R$  by  $z'=z+iz_0$  and  $R'=\sqrt{x^2+y^2+(z+iz_0)^2}$ , respectively, in the expressions for the electric dipole radiation fields Eqs. (6) and (7). For the sake of brevity, we omit the constant coefficient  $c^2\mu_0/4\pi$  in the electric and magnetic fields. Then the electromagnetic field can be expressed as

$$\vec{E}'=[(-g_1+x^2g_2)\vec{e}_x+xyg_2\vec{e}_y+x(z+iz_0)g_2\vec{e}_z], \quad (\text{A1})$$

$$\vec{B}'=\mu_0\vec{H}'=\frac{1}{c}\left\{\frac{g_1}{R'}-\frac{[P]}{R'^4}\right\}[-(z+iz_0)\vec{e}_y+y\vec{e}_z], \quad (\text{A2})$$

where

$$g_1=\frac{[\dot{p}]}{c^2R'}+\frac{[\dot{p}]}{cR'^2}+\frac{[p]}{R'^3}, \quad (\text{A3})$$

$$g_2=\frac{[\ddot{p}]}{c^2R'^3}+\frac{3[\dot{p}]}{cR'^4}+\frac{3[p]}{R'^5}. \quad (\text{A4})$$

The time factor of each physical quantity written in shortened form with brackets indicates the retarded time  $t-R'/c$ . For any oscillating form of the electric dipoles, we can obtain the following expressions:

$$\begin{aligned} \frac{\partial R'}{\partial x_i} &= \frac{x_i}{R'}, & \frac{\partial [P]}{\partial x_i} &= -\frac{x_i}{cR'}[\dot{P}], \\ \frac{\partial [\dot{p}]}{\partial x_i} &= -\frac{x_i}{cR'}[\ddot{P}], & \frac{\partial [\ddot{p}]}{\partial x_i} &= -\frac{x_i}{cR'}[\overset{\cdot\cdot}{P}], \end{aligned} \quad (\text{A5})$$

where  $x_i$  can be replaced by  $x$ ,  $y$ , and  $z+iz_0$ , respectively. From Eqs. (A3) and (A4) we can derive the following relations:

$$\frac{\partial g_1}{\partial x_i} = -x_i g_3, \quad (\text{A6})$$

$$\frac{\partial B'_x}{\partial t} = 0,$$

$$\frac{\partial g_2}{\partial x_i} = -x_i g_4, \quad (\text{A7})$$

$$\frac{\partial B'_y}{\partial t} = -(z + iz_0) \left\{ \frac{[\ddot{p}]}{c^3 R'^2} + \frac{[\dot{p}]}{c^2 R'^3} \right\},$$

where

$$g_3 = \frac{[\ddot{p}]}{c^3 R'^2} + \frac{2[\dot{p}]}{c^2 R'^3} + \frac{3[p]}{c R'^4} + \frac{3[p]}{R'^5}, \quad (\text{A8})$$

$$\frac{\partial B'_z}{\partial t} = y \left\{ \frac{[\ddot{p}]}{c^3 R'^2} + \frac{[\dot{p}]}{c^2 R'^3} \right\}. \quad (\text{A13})$$

$$g_4 = \frac{[\ddot{p}]}{c^3 R'^4} + \frac{6[\dot{p}]}{c^2 R'^5} + \frac{15[p]}{c R'^6} + \frac{15[p]}{R'^7}. \quad (\text{A9})$$

From Eqs. (A10)–(A13), we can derive the following expressions:

Using  $\partial/\partial(z + iz_0) = \partial/\partial z$ , the electromagnetic field can be obtained from Eqs. (A6)–(A9) as follows:

$$\vec{\nabla} \cdot \vec{E}' = \frac{\partial E'_x}{\partial x} + \frac{\partial E'_y}{\partial y} + \frac{\partial E'_z}{\partial z} = 4xg_2 + xg_3 - xR'^2 g_4 = 0, \quad (\text{A14})$$

$$\frac{\partial E'_x}{\partial x} = xg_3 - x^3 g_4 + 2xg_2,$$

$$\frac{\partial E'_z}{\partial y} - \frac{\partial E'_y}{\partial z} = -\frac{\partial B'_x}{\partial t} = 0, \quad (\text{A15})$$

$$\frac{\partial E'_x}{\partial y} = yg_3 - x^2 y g_4,$$

$$\frac{\partial E'_x}{\partial z} - \frac{\partial E'_z}{\partial x} = (z + iz_0)(g_3 - g_2)$$

$$\frac{\partial E'_x}{\partial z} = (z + iz_0)g_3 - x^2(z + iz_0)g_4, \quad (\text{A10})$$

$$= (z + iz_0) \left\{ \frac{[\ddot{p}]}{c^3 R'^2} + \frac{[\dot{p}]}{c^2 R'^3} \right\} = -\frac{\partial B'_y}{\partial t}, \quad (\text{A16})$$

$$\frac{\partial E'_y}{\partial x} = yg_2 - x^2 y g_4,$$

$$\frac{\partial E'_y}{\partial x} - \frac{\partial E'_x}{\partial y} = y(g_2 - g_3) = -y \left\{ \frac{[\ddot{p}]}{c^3 R'^2} + \frac{[\dot{p}]}{c^2 R'^3} \right\} = -\frac{\partial B'_z}{\partial t}. \quad (\text{A17})$$

$$\frac{\partial E'_y}{\partial y} = xg_2 - xy^2 g_4,$$

$$\frac{\partial E'_y}{\partial z} = -xy(z + iz_0)g_4, \quad (\text{A11})$$

From Eqs. (A14)–(A17) we obtained two expressions for Maxwell's equations:

$$\frac{\partial E'_z}{\partial x} = (z + iz_0)g_2 - x^2(z + iz_0)g_4,$$

$$\vec{\nabla} \cdot \vec{E}' = 0, \quad (\text{A18})$$

$$\frac{\partial E'_z}{\partial y} = -xy(z + iz_0)g_4,$$

$$\vec{\nabla} \times \vec{E}' = -\frac{\partial \vec{B}'}{\partial t}.$$

$$\frac{\partial E'_z}{\partial z} = xg_2 - x(z + iz_0)^2 g_4, \quad (\text{A12})$$

and

The other two expressions for Maxwell's equations can be verified in a similar way. Therefore, the electromagnetic fields emitted by electric dipoles in the complex-source-point model still satisfy Maxwell's equations.

- [1] H. Morgner, F. Kärtner, J. Fujimoto, E. Ippen, V. Scheuer, G. Angelow, and T. Tschudi, *Opt. Lett.* **24**, 411 (1999).  
 [2] D. H. Sutter, G. Steinmeyer, L. Gallmann, N. Matuschek, F. Morier-Genoud, U. Keller, V. Scheuer, M. Tilsch, and T. Tschudi, *Opt. Lett.* **24**, 631 (1999).  
 [3] R. Ell, U. Morgner, F. Kärtner, J. Fujimoto, E. Ippen, V. Scheuer, G. Angelow, T. Tschudi, M. Lederer, A. Boiko, and B. Luther-Davies, *Opt. Lett.* **26**, 373 (2001).

- [4] T. Brabec and F. Krausz, *Rev. Mod. Phys.* **72**, 545 (2000).  
 [5] A. E. Kaplan, S. F. Straub, and P. L. Shkolnikov, *Opt. Lett.* **22**, 405 (1997).  
 [6] G. P. Agrawal, *Nonlinear Fiber Optics* (Academic, San Diego, CA, 1995).  
 [7] J. E. Rothenberg, *Opt. Lett.* **17**, 1340 (1992).  
 [8] J. K. Ranka and A. L. Gaeta, *Opt. Lett.* **23**, 534 (1998).  
 [9] A. L. Gaeta, *Phys. Rev. Lett.* **84**, 3582 (2000).

- [10] M. A. Porras, *J. Opt. Soc. Am. B* **16**, 1468 (1999).
- [11] R. W. Hellwarth and P. Nouchi, *Phys. Rev. E* **54**, 889 (1996).
- [12] S. Hunsche, S. Feng, H. G. Winful, A. Leitenstorfer, M. C. Nuss, and E. P. Ippen, *J. Opt. Soc. Am. A* **16**, 2025 (1999).
- [13] S. Feng, H. G. Winful, and R. W. Hellwarth, *Phys. Rev. E* **59**, 4630 (1999).
- [14] R. W. Ziolkowski, *Phys. Rev. A* **39**, 2005 (1989).
- [15] R. K. Wangsness, *Electromagnetic Fields* (Wiley, New York, 1979).
- [16] E. A. Power and T. Thirunamachandran, *Proc. R. Soc. London, Ser. A* **457**, 2757 (2001); **457**, 2779 (2001).
- [17] G. A. Deschamps, *Electron. Lett.* **7**, 684 (1971).
- [18] L. B. Felsen, *J. Opt. Soc. Am.* **66**, 751 (1976).
- [19] A. L. Cullen and P. K. Yu, *Proc. R. Soc. London, Ser. A* **366**, 155 (1979).
- [20] A. E. Siegman, *J. Opt. Soc. Am.* **63**, 1093 (1973).
- [21] R. W. Ziolkowski, *J. Math. Phys.* **26**, 861 (1985).
- [22] C. J. R. Sheppard and S. Saghafi, *Optik (Stuttgart)* **110**, 487 (1999).
- [23] C. J. R. Sheppard and S. Saghafi, *J. Opt. Soc. Am. A* **16**, 1381 (1999).
- [24] C. J. R. Sheppard and S. Saghafi, *Opt. Lett.* **24**, 1543 (1999).
- [25] Z. Y. Wang, Z. Q. Zhang, Z. Z. Xu, and Q. Lin, *Int. J. Quantum Chem.* **33**, 566 (1997).
- [26] E. Heyman and L. B. Felsen, *IEEE Trans. Antennas Propag.* **AP-34**, 1062 (1986).
- [27] A. E. Kaplan, *J. Opt. Soc. Am. B* **15**, 951 (1998).